

# Measuring microlymphatic flow using fast video microscopy

## J. Brandon Dixon

Texas A&M University  
Department of Biomedical Engineering  
Mail Stop 3120  
College Station, Texas 77843  
E-mail: dixon79@neo.tamu.edu

## David C. Zawieja Anatoliy A. Gashev

Texas A&M University  
Health Science Center  
College of Medicine  
Department of Medical Physiology  
College Station, Texas 77843-1114

## Gerard L. Coté

Texas A&M University  
Department of Biomedical Engineering  
Mail Stop 3120  
College Station, Texas 77843

**Abstract.** Despite advances in the measurement of lymphatic function, little is known about the actual velocities of flow in microlymphatic ( $\sim 100 \mu\text{m}$  diam) vessels. In this work, video microscopy and particle tracking methods are adapted and integrated with an ultra-high-speed imaging camera to obtain measurements of lymph velocities throughout the entire lymphatic contraction cycle in the rat mesentery, something that previous systems were incapable of measuring. To determine the system's accuracy, calibration experiments are conducted across the hypothesized physiologically significant range of velocities for microlymphatic flow (up to 15 mm/sec). The system shows high accuracy, less than 2% error, when comparing actual with measured velocities. Microspheres flowing through 140- $\mu\text{m}$ -diam tubing are imaged to demonstrate the system's ability to determine flow rates in these small vessels by measuring particle velocities. To demonstrate biological applicability, mesenteric microlymphatics in loops of the small intestine of three male Sprague-Dawley rats are exteriorized and imaged with the high-speed system at a rate of 500 frames/sec for several contraction sequences. Lymph velocity fluctuates cyclically with the vessel wall contractions, ranging from  $-1$  to 7 mm/sec. These rates are higher than would be possible with standard video microscopy (3.75 mm/sec maximum). © 2005 Society of Photo-Optical Instrumentation Engineers. [DOI: 10.1117/1.2135791]

Keywords: lymphatics; velocity; video microscopy.

Paper 04127RRR received Jul. 8, 2004; revised manuscript received Jun. 17, 2005; accepted for publication Jun. 27, 2005; published online Nov. 18, 2005.

## 1 Introduction

The lymphatic system is a network of vessels and nodal tissues dispersed throughout the body that plays important roles in the transport of fluid, proteins, and large particulate matter from the interstitial space in the body to the blood. Over the course of a day, about 50% of the circulating blood volume is filtered out of the capillaries and returned to the circulatory system after being absorbed by lymphatic capillaries and passing through the lymphatic system. The main factors that affect flow through the lymph system are the passive and active lymph pumps and lymphatic outflow resistance. Non-lymphatic factors can influence interstitial fluid pressure to increase lymph formation and flow such as elevated capillary pressure, decreased plasma colloid osmotic pressure, increased interstitial fluid protein, and increased permeability of the capillaries.<sup>1</sup> However, flow in many lymphatics is principally driven by the intrinsic/active lymph pump. The intrinsic lymph pump is modulated by numerous factors, including physical, neural, and humoral influences.

The vessels of the lymphatic system can be divided into three general categories: initial lymphatics, collecting lymphatics, and transport lymphatics. Lymph originates in the ini-

tial lymphatics, which are dispersed throughout the tissues. Once lymph is formed in the initial lymphatics, there are two mechanisms to propagate fluid through the lymphatic system: the intrinsic pump and the extrinsic pump. The extrinsic pump responds to both steady-state lymph volumes and unsteady initial lymph volumes to fill the initial lymphatics. The steady-state response is noted to act without contraction of the initial lymphatics<sup>2,3</sup> with the exception of the bat wing. However, collecting and transport lymphatics rely heavily on the phasic contractile nature of the intrinsic pump. Smooth muscle surrounds the sections of these lymph vessels, many of which have the capability for spontaneous contractions.<sup>2</sup> Functional units of the lymphatic vessels, known as lymphangions, are arranged in series, each separated by valves.<sup>4</sup> These valves occur every 600 to 1000  $\mu\text{m}$  in rat mesentery lymphatics.<sup>5</sup> The valves are highly competent at preventing retrograde flow, even during the presence of a comparatively high reverse pressure gradient between adjacent lymphangions. This is needed to keep unwanted fluid and proteins from re-entering into initial lymphatics and potentially into the interstitial spaces. Contractions of the smooth muscle of the lymphatic vessel wall propagate along the vessel to push lymph from one lymphangion to the next. Studies have been done on

Address all correspondence to J. Brandon Dixon, Biomedical Engineering, Texas A&M University, Mail Stop 3210, College Station, TX 77843. Tel: 979-862-1076. Fax: 979-845-4450. E-mail: dixon79@tamu.edu

the propagation of this motion, noting the phase, frequency, and amplitude of such contractions.<sup>5-7</sup>

While work in the last few decades has shed light on many aspects of lymphatic transport function, very little is known about the actual fluid velocity in the smaller (100  $\mu\text{m}$ ) microlymphatic vessels that are often highly contractile. Characterization of flow through the lymph system is important for a better understanding of how the system responds to the various changes in physical factors, such as interstitial fluid pressure, fluid volume, and lymphatic wall shear stress. There is an abundance of literature in some of these areas of lymphatic physiology.<sup>8-14</sup> The majority of the work done to date did not concern itself with the mechanisms behind such flow, but rather focused on obtaining quantitative measures of flow in the large vessels of the lymphatic system.<sup>8-11</sup>

Recently, however, researchers have been investigating the effects of various regulators on contraction frequency and amplitude<sup>12,13,15-18</sup> to better understand the physiological mechanisms intrinsic to the lymphatics system. One of the main factors shown to reduce the spontaneous transient depolarizations in the lymph vessels is nitric oxide.<sup>12,15,16,18</sup> Others have shown the effects of various endothelial prostanoids on contractile activity.<sup>13,16,19</sup> While the effects of some biochemical regulators have been extensively investigated, less is known about the mechanisms that control their release. The majority of the work done on the physical parameters that cause these biochemical regulators to be released has been in the area of transmural pressure response.<sup>6,14,20,21</sup> It is also hypothesized that fluid velocity, by means of shear stress, plays an important role in the coordination of wall contractions and lymph propagation in addition to pressure. It has been shown previously by Gashev, Davis, and Zawieja that increasing flow while holding pressure constant actually inhibits the active lymph pump both in frequency and amplitude in a manner qualitatively similar to nitric oxide.<sup>12</sup> While some groups have looked at shear stress and its ability to promote lymph flow to areas of inflammation,<sup>22</sup> little is known about the role of shear stress on the intrinsic lymph pump. This is important, as it is believed to be the underlying mechanism behind the responses to flow observed in the prior cases. Shear stress is the force that the endothelial cells of the vessel wall "feel" as the flow through the vessels increases. It is known from the study mentioned before<sup>12</sup> that shear is responsible for this effect because the transmural pressure is being held constant. To be able to accurately measure shear, measurement of the velocity profile across the diameter of the vessel wall is required and the velocity fluctuations throughout the contraction cycle need to be monitored.

## 2 Theory

In this section, a brief explanation is provided of the equations used to measure the velocity of the contractions in the lymphatic wall, the velocity of luminal lymphocytes, the diameter of the vessel, and the radial location of the lymphocytes with respect to the centerline. Currently, a three point method is used to measure the luminal diameter and provide a reference to calculate the distance of each lymphocyte from the center of the vessel (Fig. 1). The diameter of the vessel wall ( $W$ ) and distance from the centerline ( $D$ ) are calculated using Eqs. (1) and (2), given the variables as defined in Fig. 1.

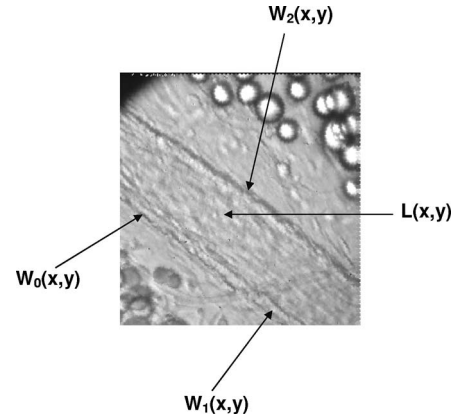


**Fig. 1** An image of a microlymphatic vessel with the measured wall coordinates ( $W_0$ ,  $W_1$ , and  $W_2$ ) and a lymphocyte at location  $[L(x, y)]$ . The field of view is roughly  $250 \times 250 \mu\text{m}$ .

In the figure,  $W_0$ ,  $W_1$ , and  $W_2$  are the three  $(x, y)$  coordinates chosen along the wall of the vessel (Fig. 1), while  $L$  is the  $(x, y)$  coordinate of a given lymphocyte (Fig. 1). Given this geometry, the vessel luminal diameter can be calculated as:

$$W = \left[ b^2 - \left( \frac{a^2 + b^2 - c^2}{2a} \right)^2 \right]^{1/2}, \quad (1)$$

in which,

$$a = \{ [W_0(x) - W_1(x)]^2 + [W_0(y) - W_1(y)]^2 \}^{1/2},$$

$$b = \{ [W_0(x) - W_2(x)]^2 + [W_0(y) - W_2(y)]^2 \}^{1/2},$$

$$c = \{ [W_1(x) - W_2(x)]^2 + [W_1(y) - W_2(y)]^2 \}^{1/2}.$$

Further, the distance of a given lymphocyte from the centerline can be calculated as:

$$D = \left[ b'^2 - \left( \frac{a^2 + b'^2 - c'^2}{2a} \right)^2 \right]^{1/2} - \frac{W}{2}, \quad (2)$$

in which,

$$b' = [W_0(x) - L(x)]^2 + [W_0(y) - L(y)]^2,$$

$$c' = [W_1(x) - L(x)]^2 + [W_1(y) - L(y)]^2.$$

The velocities of the lymphocytes ( $V_L$ ) were measured by tracking the coordinates of the lymphocyte over a sequence of images using the following equation:

$$V_L = \frac{\{ [L_{t_0}(x) - L_{t_0+\Delta t}(x)]^2 + [L_{t_0}(y) - L_{t_0+\Delta t}(y)]^2 \}^{1/2}}{\Delta t}, \quad (3)$$

in which  $L_{t_0}(x, y)$  is the position of some given lymphocyte at time  $t_0$ . The value  $L_{t_0+\Delta t}(x, y)$  is the position of the same lymphocyte at some time  $\Delta t$  past  $t_0$ , and  $\Delta t$  is the time interval between images.

The velocity of the wall contractions ( $V_w$ ) were calculated by the following equation:

$$V_w = \frac{[(W_{t_0} - W_{t_0+\Delta t})^2]^{1/2}}{\Delta t}, \quad (4)$$

in which  $W_{t_0}$  is the diameter of the vessel at time  $t_0$ . Similarly,  $W_{t_0+\Delta t}$  is the diameter of the vessel at some time  $\Delta t$  past  $t_0$ , and  $\Delta t$  is the time interval between images.

### 3 Materials and Methods

Initially, it was uncertain as to how fast the camera needed to record images. To save the images at a rate fast enough to keep pace with the camera, the images were dumped into an allocated buffer of RAM (approximately 1 GB). Once the RAM was full, the recording had to be stopped so that the images could be stored onto the hard drive. The allocation of RAM available for this allowed us to capture 6528 images before the buffer became full. A tradeoff exists between the speed of the camera and the length of continuous imaging that can be achieved. Using prior knowledge from previous studies of lymph wall contractions done by our group, it was determined that the image sequences needed to be at least 15 sec to capture several contraction cycles. The camera speed was maximized while extending the duration of the recording time to 30 sec by dividing the 6528 images into 384 sets of 17 images per set and placing a pause between each set. Within one set of 17 images, the first 16 images were captured with a 2-ms integration time per image (500 frames/sec). Image 17 was saturated by increasing the integration time of the camera to 8 ms to extend the duration of the sequence, given the limitation of RAM. This resulted in a total time of 62 ms between each set of images ( $16 \times 2 \text{ ms} + 8 \text{ ms} + 22 \text{ ms}$  memory transfer time). This allowed for the measurement of velocities up to seven times faster than the capabilities of previous imaging systems used to measure lymph velocities while still maintaining the necessary dynamic range of 30 sec to image several complete contraction cycles. These imaging parameters were set with a software interface available through Epix (XCAP-Std. V2.2, Buffalo Grove, Illinois). Lymphatic wall measurements were recorded at the beginning of every set of 17 images. This allowed us to measure wall contractions using a frame rate of 40 fps, a speed similar to that of standard 30-fps cameras and sufficient to measure wall velocity throughout the phases of the contractile cycle.

#### 3.1 Calibration Experiments

Calibration experiments were conducted to quantify the ability of the system to measure velocities at high frame rates using the capturing method described earlier. Two separate experiments were run: one to assess the sensitivity and accuracy of the velocity measurements, and another to determine the system's ability to estimate the velocity and radial position of particles moving through a tube of similar diameter to the microlymphatics. For the first set of experiments, a wheel was used that rotated at various revolutions per minute and was positioned under the microscope for imaging. The wheel consisted of a motor-driven rotating disk with markings on it at a fixed radial distance. Image sequences were recorded with the

high-speed video camera [Dalstar64K1M, 1M fps  $245 \times 245$ , charge-coupled device (CCD) camera] at a fixed radial distance (28.5 mm) on the wheel while varying the angular velocity, so that a range of velocities could be measured that would be similar to those that were expected to occur physiologically (up to 15 mm/sec). Multiple measurements were taken while maintaining a constant speed to quantify the sensitivity of such measurements.

For the second set of experiments, we designed a physical model that simulated the sizes and arrangements of lymphocytes flowing through a microlymphatic vessel using a suspension of microspheres that was passed through a glass capillary tube. A solution of sodium chloride was prepared that matched the specific gravity of the microspheres used to simulate the white blood cells. The saline solution also served to dilute the  $7.12\text{-}\mu\text{m}$ -diam microspheres to a concentration of about  $5 \cdot 10^5$  microspheres/mL, approximating the size and count of lymphocytes. A glass capillary tube was heated and pulled out to a diameter of  $140 \mu\text{m}$ , equivalent to the diastolic diameters of the lymphatic vessels we are studying. These values were chosen to mimic the dimensions that occur in the microlymphatics being measured *in situ* as closely as possible. The fluid was passed through the tubing by applying a constant pressure with a level pressure head that could be moved up and down to control pressure. The outflow resistance was set to yield velocities that are similar to those measured *in situ*. The tubing was magnified using the same microscope optics used to record the lymphatic vessels. The images were recorded at a frame rate of 500 frames/sec. Velocity measurements were made at fixed moments in time (25 ms) for a range of flow rates (15 to 250  $\mu\text{L/hr}$ ). The actual flow rate was measured by using a bubble tracking technique, and compared to the flow rates calculated from the images.

#### 3.2 In Situ Lymph Velocity Measurements

Three male Sprague-Dawley rats weighing 180 to 220 g were used for these experiments. The rats were housed in an environmentally controlled, American Association for Accreditation of Laboratory Animal Care approved vivarium. Each animal was fasted for 12 to 15 h before the experiments, while water was available *ad libitum*. Each rat was anesthetized with an intramuscular injection of Fentanyl-Droperidol (0.3 mL/kg) and Diazepam (2.5 mg/kg). Supplemental doses of the anesthetic were given as needed. An abdominal incision was made to gain access to the mesenteric lymphatic vessels. A loop of the small intestine was exteriorized through the incision and gently positioned over a semicircular viewing pedestal on a Plexiglas preparation board. A lymphatic vessel was centered over an optical window in the preparation board. The exteriorized tissue was perfused with a phosphate buffered solution supplemented with HEPES (10 mM) and 1% bovine serum albumin. The solution was prewarmed to  $38^\circ\text{C}$ , and the pH adjusted to 7.4. The temperature of the exteriorized tissue and the animal's core were maintained at  $36$  to  $38^\circ\text{C}$ . The preparation board was placed on the stage of an intravital microscope (Zeiss), and the lymphatic vessel was observed at a magnification of 100 to  $200\times$  using an 80-mm projective lens, a  $10\times$  water immersion objective, and a variable magnification intermediate lens. The depth of

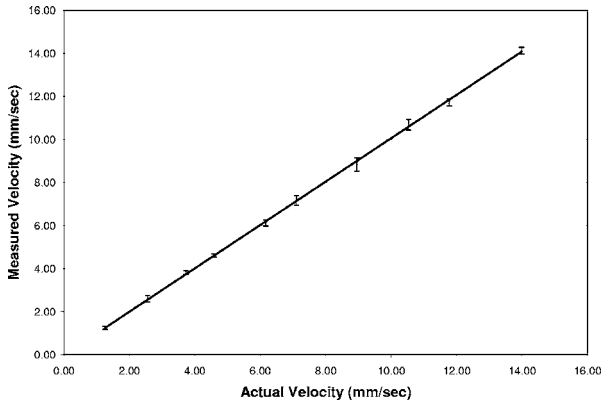


**Fig. 2** Actual versus measured velocities of *in vitro* calibration wheel with error bars.

field for this optic setup was approximately  $14\ \mu\text{m}$ . All the experiments were digitized with the high-speed video camera (Dalstar64K1M, 1M fps  $245 \times 245$ , CCD camera) using the capturing technique described previously. After imaging and recording the specimen, the image sequences were loaded for analysis in Epix, an image analysis software package using the three point measuring method described in Sec. 2. To record the wall measurements, a sequence of images was loaded through a program written in Matlab, and three coordinates were selected with a cursor along the wall, as shown in Fig. 1. This was done for sets of 51 images for the entire sequence of 6258 images. This ensured that the luminal diameter was being measured at the same location for the entire recording sequence. These coordinates were then imported into a program to make all of the necessary calculations. Lymphocytes were tracked manually by recording the location of the coordinates of the lymphocyte. An arbitrary lymphocyte within the field of view and depth of focus was chosen, and that particle was tracked for 24 ms. Software was developed to import these coordinates and calculate the lymphocyte velocity, the distance of the particle from the centerline, and the volume flow rate.

## 4 Results and Discussion

### 4.1 Calibration Experiments

Calibration experiments were conducted to ensure the accuracy of the camera timing and our velocity estimation procedure. The calibration wheel was imaged at ten different velocities three times each, and the velocities were calculated from the images and compared with the actual velocity of the wheel to test for system accuracy and sensitivity. Figure 2 shows the actual versus measured velocities for all measurements ( $R^2=0.999$ ). The system showed accuracy with less than 2% error when compared to actual velocities, and a sensitivity that yielded an average standard deviation of  $\sim 0.17\ \text{mm/sec}$  for multiple measurements at a given velocity.

For the second set of calibration experiments, images were recorded while flowing fluid and microspheres through a synthetic vessel. Velocities and the distance of the particles from the centerline were measured five different times throughout the sequence of flow for eight different flow rates. Figure 3

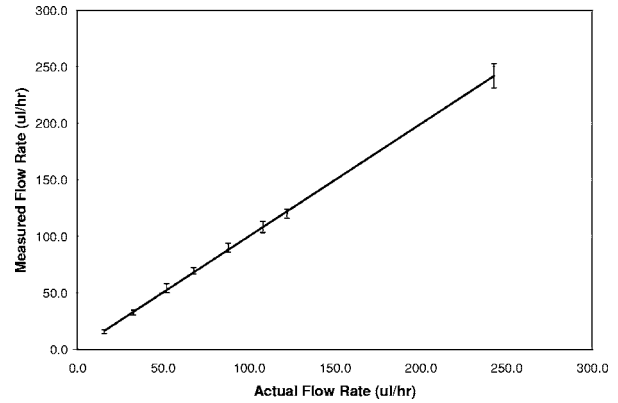


**Fig. 3** Actual versus measured volume flow rates of microspheres flowing through  $140\text{-}\mu\text{m}$  glass tube.

shows the actual versus average predicted flow rates for each of the eight measurements along with error bars ( $R^2=0.999$ ). Since the Reynolds number is very small ( $<5$ ), the volume flow rate could be calculated from the particle's velocity and position given by Eq. (5), which is derived from Navier-Stokes for laminar flow through a tube ( $Q$ =volume flow rate,  $V_{\bar{r}}$ =velocity of particle measured at some distance  $\bar{r}$  from the center,  $r$ =vessel radius).

$$Q = \frac{\pi V_{\bar{r}} r^4}{2(r^2 - \bar{r}^2)}. \quad (5)$$

This approximation resulted in an average error of 5.7% with a maximum error of 10.6%. This is more than likely due to the depth of field covering more than just the center of the vessel, resulting in error in the distance from the centerline measurements. However, it was within acceptable limits to make reasonable estimations of *in situ* flow rates.

### 4.2 In Situ Experiments

Preliminary results for several contractions for three different rats have shown the viability of this system to measure the velocity in the microlymphatic vessel of the rat while simultaneously recording the diameter of the vessel [Figs. 4(a)–4(c)]. Lymphocytes velocities ranged from  $-1$  to  $7\ \text{mm/sec}$ . As can be seen by the three figures, the pattern and dynamic range of the diameters and the contraction frequencies varied from rat to rat. Quantitative measurements of fluid velocities in the microlymphatics were recorded through the entire contraction cycle and fast video microscopy was used to measure velocities greater than  $1\ \text{mm/sec}$  for the first time. As expected, the velocity of the lymph fluid fluctuates in a cyclical pattern at the same frequency as the wall contractions with a slight phase difference. The range of values measured for the lymphocyte velocities is much larger than previous systems were capable of measuring using standard video microscopy. For example, the typical field of view when applying the necessary magnification to these vessels is  $250 \times 250\ \mu\text{m}$ . To track a particle, one must measure that particle's location at two different times. This means that the particle can travel no further than  $125\ \mu\text{m}$  to ensure that the particle is captured twice before it leaves the field of view. Therefore, the maximum velocity a

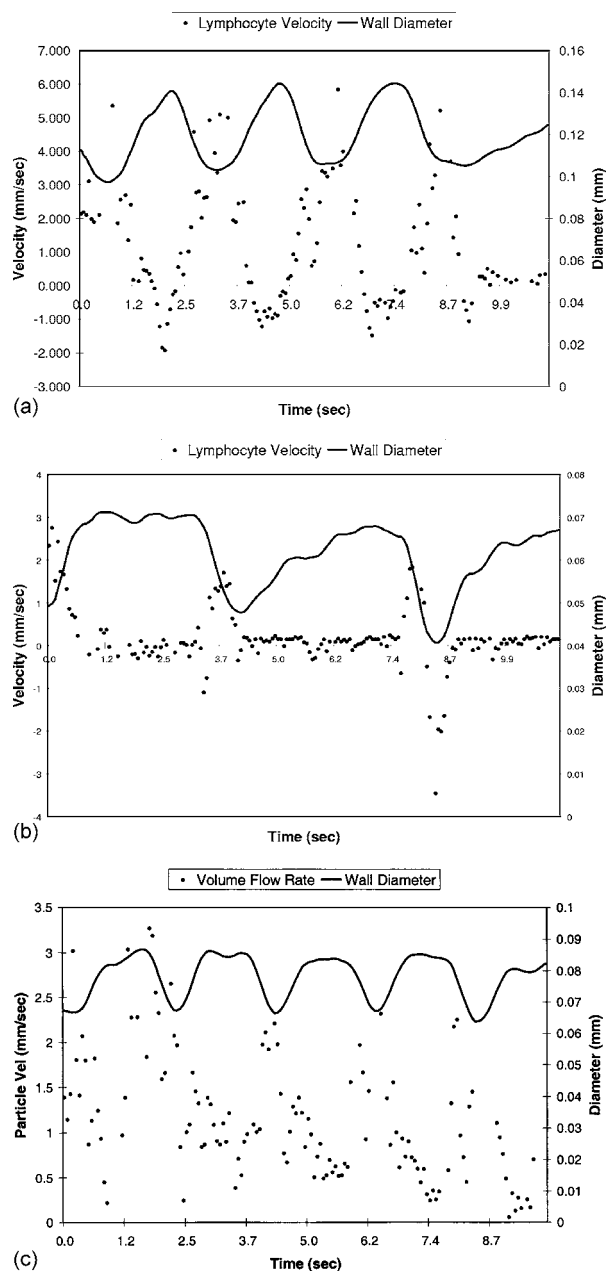


**Fig. 4** (a), (b), and (c) Vessel lumen diameter (mm) and lymphocyte velocity (mm/sec) for 10-sec intervals for three rats.

30 frame/sec camera could theoretically measure is 3.75 mm/sec (velocity=distance/time= $125\ \mu\text{m}/0.033\ \text{s}$ ). This is under an ideal scenario in which one could resolve the  $125\ \mu\text{m}$  “streak” that would occur as a result of the moving particle when imaging at 30 fps (assuming that you are not electronically shuttering). This is illustrated by the images shown in Figs. 5(a)–5(c). These images were taken during the peak velocity measurement at time  $t=6.08\ \text{sec}$  from Fig. 4(a), which is during a peak velocity measurement of 5.8 mm/sec (larger than the 3.75-mm/sec limit). As seen by comparing Figs. 5(a) and 5(b), which occur 2 ms apart, both particles appear in the field of view. However, in Fig. 5(c), taken 33 ms after Fig. 5(a), neither lymphocyte is in the field of view. It should be noted that each image has been subtracted from the

image immediately following it to remove the background and enhance objects in motion. Coordinates of the lymphocyte are also shown to illustrate the displacement of the lymphocyte from Figs. 5(a) and 5(b). In conclusion, a conventional 30-fps imaging system is too slow, given the velocities that we have measured *in situ*.

The maximum contractions observed in the microlymphatics of rats can be 60%, with average contractions being approximately 40 to 50% of the vessel diameter.<sup>5</sup> In this particular set of rats, the contractions were about 40% of the maximum diameter. This would lead one to believe that in vessels with even larger contractions, the maximum velocities observed would be even greater than the 7 mm/sec observed in this case, further emphasizing the need for a fast imaging system. Figure 6 shows the estimated volume flow rate from the datasets shown in Fig. 4(a). Similar plots can be generated from our measurements shown in Figs. 4(b) and 4(c).

There have been several other techniques that have been developed over the years to quantify flow and map out the structure of both blood and lymphatic flow.<sup>3,8–14,23–36</sup> The most common approaches include fluorescence techniques,<sup>9,11,14,23,24,37,38</sup> Doppler Flowmetry,<sup>27–36</sup> and video microscopy.<sup>5,10,16,18,20–22,39–41</sup> While fluorescent techniques are useful in obtaining bulk flow information, one big disadvantage is that injection is often difficult in smaller vessels, and the introduction of foreign fluorescent particles into the system is likely to alter the contraction cycle that normally occurs physiologically.

While Doppler methods have been used with microscopy to measure flow for over 30 years,<sup>27</sup> flow through lymph vessels has proved to be more difficult, as the method is dependent on the presence of numerous scatterers flowing through the system. In most lymphatic vessels, the presence of particles, particularly white blood cells, is much scarcer than red blood cells in the blood. The velocity patterns in lymphatic capillaries are also much more complicated due to the presence of backflow and multiple valves, as discussed previously. These complications make a Doppler approach much more difficult for the lymphatic system than for blood flow measurements. However, one group has successfully used a Doppler-based approach to acquire direct measurements of lymph flow in the posterior lymph heart of toads.<sup>36</sup> In this specific case, many of the disadvantages discussed before do not occur, as the lymphatic systems of most amphibians behave more like the circulatory system with a pumping organ pushing flow through the vessels.

Video microscopy analysis has long been the gold standard for imaging flow through vessels and measuring vessel diameter.<sup>5,10,14,21,22,39–41</sup> The technology itself has existed for many decades; however, recent developments in computing speed have allowed for more exhaustive image analysis algorithms to be developed. Almost all applications of such systems for lymph flow have been captured with a standard video camera at a rate of 30 frames/sec. This has proved acceptable for measurements in contraction speed and average lymph flow, as the velocities that occur in such cases are not beyond the speed of the camera (less than 1 mm/sec for microlymphatic flow, given a magnification of around 100 to 200 $\times$ ). However, our group observed in initial experiments highly blurred particles during contractions that indicated that veloci-

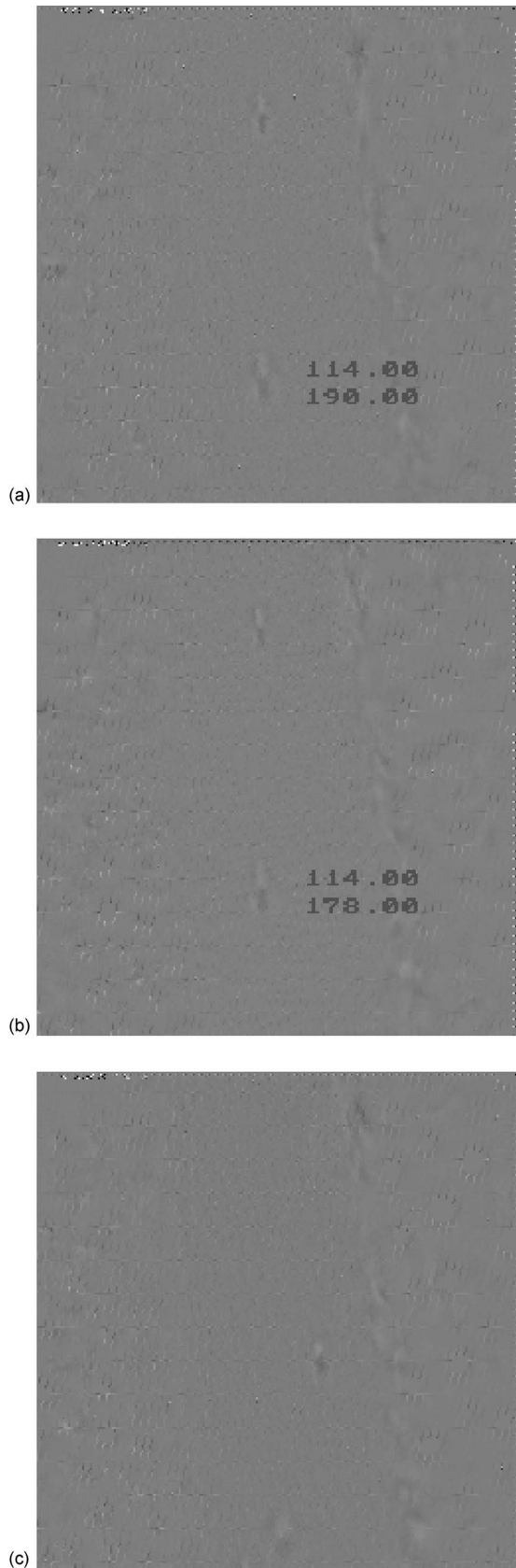


**Fig. 5** (a) *In situ* image taken during 5.8 mm/sec fluid flow at time  $t = 0$ . The coordinates correspond to the lower lymphocyte. (b) *In situ* image taken at time  $t = 2$  ms. The lymphocyte has moved 12 pixels. (c) *In situ* image taken at time  $t = 33$  ms. Neither lymphocyte is present in the image; however, new ones have appeared.

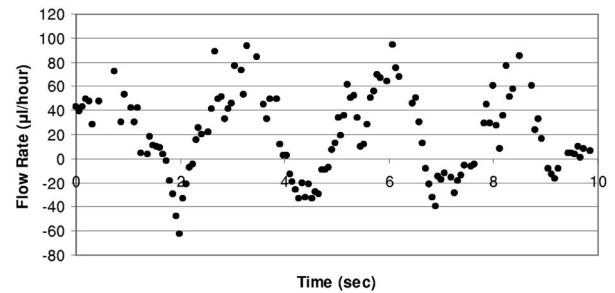


**Fig. 6** Estimation of volume flow rates ( $\mu\text{L/hr}$ ) from velocity data in Fig. 4(a).

ties of local flow during the phasic contractions are much higher than those that current video systems are capable of measuring. For example, a particle moving at 7 mm/sec, if imaged with a conventional video microscopy system, would in theory be a blurred streak of about  $250 \mu\text{m}$  in length. The problem is that the contrast between white blood cells and the lymph media is so poor given the complex *in situ* image that the length of this streak cannot be measured, or even seen in some cases, and the velocity cannot be deduced. Therefore, we pursued the use of a high-speed camera, using capture rates of up to 500 frames/sec, to measure these higher-end velocities. The advantage of this system is the ability for excellent resolution, both temporally and spatially.

## 5 Conclusions

There are currently a wide variety of imaging methods available for measuring lymph flow, each with their own advantages and disadvantages. With the recent developments in camera speed and the constant improvements in computer performance, some of the limitations that existed in the past for lymphatic imaging were shown to be removed in this work. The *in situ* data presented here correspond to three segments of 10 sec of continuous contractions in three different rats to show the feasibility of the system to accurately measure the higher-end velocities that occur, as well as to provide some verifiable data that such velocities exist. Through the unique image acquisition process presented, adequate data were collected for the first time to measure fluid velocity throughout the entire contraction cycle while maximizing the hardware resources currently available for acquisition. Initial studies have shown velocities up to 7 mm/sec, which appear to occur immediately following the onset of vessel contraction. The postprocessing methods developed have been sufficient to measure the velocity, diameter, and distance of the lymphocyte from the centerline. There is room for improvements in this approach, including automated postprocessing and ample room for further investigation with this technique. In particular, continued analysis of multiple rats will need to be undertaken to produce more statistically significant results in regard to the correlation between contraction strength and frequency with fluid flow and shear.

## Acknowledgments

NIH grant HL-070308 and the Whitaker Foundation Special Opportunity Grant.

## References

1. A. Guyton and J. Hall, *Textbook of Medical Physiology*, 9th ed., W.B. Saunders Company, Philadelphia, PA (1996).
2. M. Muthuchamy, A. Gashev, N. Boswell, N. Dawson, and D. Zawieja, "Molecular and functional analyses of the contractile apparatus in lymphatic muscle," *FASEB J.* **20** (2003).
3. G. Schmid-Schönbein, "Microlymphatics and lymph flow," *Physiol. Rev.* **70**, 987–1028 (1990).
4. H. Mislin and R. Schipp, "Structural and functional relations of the mesenteric lymph vessels," *Progress in Lymphology*, A. Rüttimann, Ed., pp. 360–365, Hafner, New York (1967).
5. D. Zawieja, K. Davis, R. Schuster, M. Hinds, and H. Granger, "Distribution, propagation, and coordination of contractile activity in lymphatics," *Am. J. Physiol.* **264**, H1283–H1291 (1993).
6. N. McHale and I. Roddie, "The effect of transmural pressure on pumping activity in isolated bovine lymphatic vessels," *J. Physiol. (London)* **261**, 255–269 (1976).
7. N. G. McHale and M. K. Meharg, "Co-ordination of pumping in isolated bovine lymphatic vessels," *J. Physiol. (London)* **450**, 503–512 (1992).
8. M. Fischer, U. Costanzo, U. Hoffman, A. Bollinger, and U. Franzeck, "Flow velocity of cutaneous lymphatic capillaries in patients with primary lymphedema," *Int. J. Microcirc.: Clin. Exp.* **17**, 143–149 (1997).
9. M. Fischer, U. Franzeck, I. Herrig, U. Costanzo, S. Wen, M. Shiesser, U. Hoffmann, and A. Bollinger, "Flow velocity of single lymphatic capillaries in human skin," *Am. J. Physiol.* **270**, H358–H363 (1996).
10. S. Baez, "Flow properties of lymph—A microcirculation study," *Flow Properties of Blood and Other Biological Systems*, Pergamon Press, New York (1960).
11. A. Leu, D. Berk, F. Yuan, and R. Jain, "Flow velocity in the superficial lymphatic network of the mouse tail," *Am. J. Physiol.* **267**, H1507–H1513 (1994).
12. A. Gashev, M. Davis, and D. Zawieja, "Inhibition of the active lymph pump by flow in rat mesenteric lymphatics and thoracic duct," *J. Physiol. (London)* **540**, 1023–1037 (2002).
13. K. John and A. Barakat, "Modulation of ATP/ADP concentration at the endothelial surface by shear stress: effect of flow-induced ATP release," *Ann. Biomed. Eng.* **29**, 740–751 (2001).
14. W. Olszewski and A. Engeset, "Intrinsic contractility of prenodal lymph vessels and lymph flow in human leg," *Am. J. Physiol.* **239**, H775–H783 (1980).
15. P. Von der Weid, J. Zhao, and D. Van Helden, "Nitric oxide decrease pacemaker activity in lymphatic vessels of guinea pig mesentery," *Am. J. Physiol.* **280**, H2707–H2716 (2001).
16. R. Mizuno, A. Koller, and G. Kaley, "Regulation of the vasomotor activity of lymph microvessels by nitric oxide and prostaglandins," *Am. J. Physiol.* **274**, R790–R796 (1998).
17. H. Sakai, F. Ikomi, and T. Ohhashi, "Effects of endothelin on spontaneous contractions in lymph vessels," *Am. J. Physiol.* **277**, H459–H466 (1999).
18. Y. Shirasawa, F. Ikomi, and T. Ohhashi, "Physiological roles of endogenous nitric oxide in lymphatic pump activity of rat mesentery in vivo," *Am. J. Physiol.* **278**, G551–G556 (2000).
19. N. Reddy, "Lymph circulation: Physiology, pharmacology, and biomechanics," *Crit. Rev. Biomed. Eng.* **14**, 45–91 (1986).
20. A. Hargens and B. Zweifach, "Contractile stimuli in collecting lymph vessels," *Am. J. Physiol.* **233**, H57–H65 (1977).
21. J. Benoit, D. Zawieja, A. Goodman, and H. Granger, "Characterization of intact mesenteric lymphatic pump and its responsiveness to acute edemagenic stress," *Am. J. Physiol.* **257**, H2509–H2069 (1989).
22. X. Li, M. Su, C. West, C. He, S. Swanson, T. Secomb, and S. Mentzer, "Effect of shear stress on efferent lymph-derived lymphocytes in contact with activated endothelial monolayers," *In Vitro Cell Dev. Biol.* **37**, 599–605 (2001).
23. M. Swartz, D. Berk, and R. Jain, "Transport in lymphatic capillaries. I. Macroscopic measurements using residence time distribution theory," *Am. J. Physiol.* **270**, H324–H329 (1996).
24. D. Berk, M. Swartz, A. Leu, and R. Jain, "Transport in lymphatic capillaries. II. Microscopic velocity measurement with fluorescence photobleaching," *Am. J. Physiol.* **270**, H330–H337 (1996).
25. W. Svennson, D. Glass, D. Bradley, and A. Peters, "Measurement of lymphatic function with technetium-99m-labelled polyclonal immunoglobulin," *Eur. J. Nucl. Med.* **26**, 504–510 (1999).
26. C. Witte, M. Witte, A. Unger, W. Williams, M. Bernas, G. McNeill, and A. Stazzone, "Advances in imaging of lymph flow disorders," *Radiographics* **20**, 1697–1719 (2000).
27. H. Mishina and T. Asakura, "A laser doppler microscope," *Opt. Commun.* **11**, 99–102 (1974).
28. G. E. Nilsson, T. Tenland, and P. A. Oberg, "Evaluation of a laser Doppler flowmeter for measurement of tissue blood flow," *IEEE Trans. Biomed. Eng.* **27**, 597–604 (1980).
29. R. Bonner and R. Nossal, "Model for laser Doppler measurements of blood flow in tissue," *Appl. Opt.* **20**, 2097–2107 (1981).
30. R. Lohwasser and G. Soelkner, "Experimental and theoretical laser-Doppler frequency spectra of a tissuelike model of a human head with capillaries," *Appl. Opt.* **38**, 2128–2137 (1999).
31. J. Steinbrink, H. Wabnitz, H. Obrig, A. Villringer, and H. Rinneberg, "Determining changes in NIR absorption using a layered model of the human head," *Phys. Med. Biol.* **46**, 879–896 (2001).
32. H. Liu, "Development of a brain spectrometer for guiding brain surgery and in vivo monitoring of cerebral oxygenation," <http://www.whitaker.org/abstracts/rgapr97.html> (2002).
33. Z. Chen, "Optical Doppler tomography for high resolution imaging of in vivo microcirculation," <http://www.whitaker.org/abstracts/rgapr97.html> (2002).
34. Moor Instruments, "Burn depth assessment by laser Doppler imaging," <http://www.moor.co.uk/pdf/burns.pdf> (1998).
35. C. M. Choi and R. G. Bennett, "Laser dopplers to determine cutaneous blood flow," *Dermatol. Surg.* **29**, 272–280 (2003).
36. J. Jones, A. Gamperl, A. Farrell, and D. Toews, "Direct measurement of flow from the posterior lymph hearts of hydrated and dehydrated toads (*Bufo Marinus*)," *J. Exp. Biol.* **200**, 1695–1702 (1997).
37. F. Mahler, C. Boss, and H. Saner, "Microlymphography with FITC human albumin," *The Initial Lymphatics, New Methods and Findings*, pp. 106–109, Thieme, New York (1985).
38. A. Bollinger and B. Fagrell, *Clinical Capillaroscopy, a Guide to Its Use in Clinical Research and Practice*, Hogrefe Huber, Lewiston, NY (1990).
39. T. Neild, "Analysis of arteriole diameter changes by analysis of television images," *Blood Vessels* **26**, 48–52 (1989).
40. B. Fagrell, A. Fronek, and M. Intaglietta, "A microscope-television system for studying flow velocity in human skin capillaries," *Am. J. Physiol.* **233**, H318–H321 (1977).
41. G. Sainte-Marie, F. Peng, and C. Bélisle, "Overall architecture and pattern of lymph flow in the rat lymph node," *Am. J. Anat.* **164**, 275–309 (1982).